CONFORMAL ANTENNAS

A conformal antenna may be defined as an antenna whose radiating aperture conforms to the surface of the body on which it is mounted. Ideally, such antennas are flush mounted or low profile (i.e., they do not protrude appreciably out of the mounting surface). Basic slot and microstrip (patch) antennas are typical examples of conformal antenna elements. The term *conformal array* has no unique definition. Kummer (1) defines it as an array that is nonplanar. We shall assume here that a conformal array consists of conformal (or low-profile) antenna elements placed on a nonplanar surface. The array surface is not generally at the disposal of the antenna designer and is often dictated by the specific application. For ground-based application, a conformal phased array requiring coverage over 360° in azimuth (omnidirectional coverage) or coverage over a hemisphere the array surface may be cylindrical or spherical, respectively. For conformal arrays on aircraft, missiles, satellites, and surface ships, the array shape may assume another form dictated by the contour of the vehicle. Basic slot and microstrip antennas are extensively discussed in the literature—for example, the textbook by Balanis (2) is a typical reference. These antennas provide ideal performance only when they are mounted on planar surfaces. During conformal application the curvature of the mounting surface can affect their impedance and radiation properties; such effects must be taken into account during the design of such antennas.

The need for conformal phased arrays for aircraft and missile applications, and for ground-based arrays with omnidirectional coverage in azimuth or complete hemispherical coverage in space, has grown continually with requirements that emphasize maximum utilization of available space and minimum cost. Many of the developments in conformal arrays have been extensions of the concepts for planar phased arrays, which are extensively discussed in the literature (for example, in Ref. 2). However, there are significant differences between planar and conformal arrays that must be taken into account during the design of the latter. The individual elements on curved bodies point in different directions that make it necessary to turn off those elements that radiate primarily away from the desired beam direction. For this reason also, one cannot factor out the element pattern out of the total radiation pattern—this makes the conformal array analysis and synthesis more difficult. The element orientation may also cause severe crosspolarization. In addition, the mutual coupling effects between the elements can be severe in some cases.

Within the limitations of space allowed, it is not possible to describe here every aspect of conformal antennas and antenna arrays. Instead, we shall at first describe briefly certain aspects of a few basic antennas that are commonly used either singly or as array elements for conformal applications. Then we give brief descriptions of a selected number of conformal antennas and antenna arrays. Specifically, this article describes the following:

1. The specific considerations that must be given to the performance of basic slot and microstrip or patch antenna elements when mounted on nonplanar conducting surfaces
2. A selected number of conformal antennas: for example, microstrip conformal antennas and dielectric filled edge slot (DFES) antennas
3. A class of wraparound antennas and antenna arrays
4. Cylindrical and spherical phased arrays used for omnidirectional and hemisphereical coverage, respectively.

All of the aforementioned antennas have found practical applications. Detailed descriptions of their development, design procedures, and analysis of their performance are described in the references cited at appropriate places.

Literature on conformal antennas is vast and ranges from technical journal articles to numerous textbooks and specialized books, of which Refs. 2–8 are typical.

BASIC ANTENNA ELEMENTS

Elementary slot and microstrip patch antennas are commonly used singly or as array elements for conformal application. However, these radiators provide ideal performance only when they use plane conducting surfaces. Ideal theory can be used when the radii of curvature of the surfaces are large compared to the operating wavelength. In other cases both the impedance and radiation characteristics may be affected significantly.

Slots on Curved Surfaces

The radiation patterns of slot antennas can be significantly altered by the curved mounting surface. Pathak and Kouyoumjian (9) give a convenient extension of the geometrical theory of diffraction (GTD) for apertures in curved surfaces.

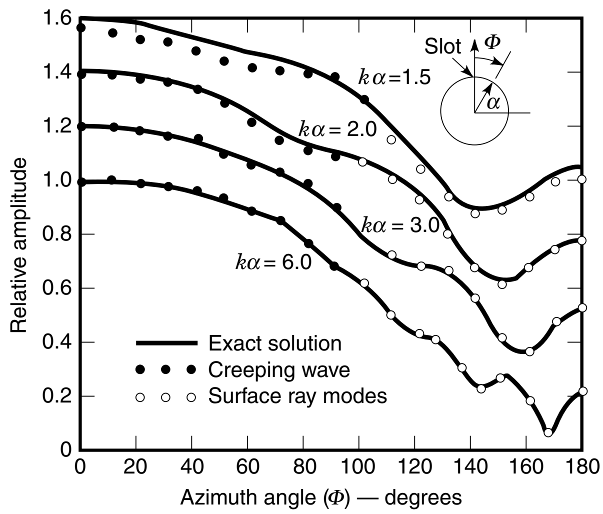

Figure 1. Patterns of a thin axial slot on a perfectly conducting cylinder. (After Ref. 9.)

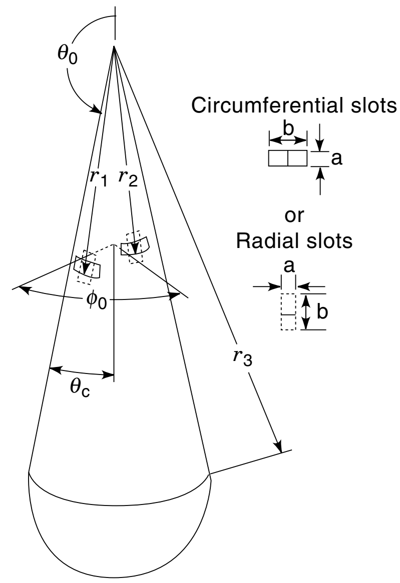

Figure 3. Slotted cone geometry.

Figure 1, taken from Ref. 9, shows the patterns of an axial slot element on perfectly conducting circular cylinders of various radii; the results indicate the accuracy of the approximate theory. The effects of the cylinder radius on the patterns shown in Fig. 1 should be noticed. A similar slot on a flat ground plane would have a constant pattern from $\phi = 0$ to 180°. Radiation patterns of slots on a variety of other generalized surfaces are discussed in Refs. 10–12. Mailloux (13) summarizes some of the results of Pathak and Kouyoumjian (9) shown in Fig. 2, which gives the radiated power pattern in the upper half plane ($\theta \leq 90°$) for an infinitesimal slot in a cylinder of radius a. The angular extent of the transition zone is on the order of $(k_0a)^{-1/3}$ on each side of the shadow boundary, $k_0 = 2\pi/\lambda_0$ being the propagation constant in free space. The results indicate that above the transition zone (i.e., the illuminated zone) the circumferentially polarized radiation is nearly constant but the axially polarized radiation has a cos θ pattern. Compared with the field strength in the $\theta = 0°$ direction, the field strengths in the $\theta = 90°$ area are found to be about 0.7 and $0.4(2/k_0a)^{1/3}$ for circumferential and axial polarizations, respectively. It should be noted that in the case of flat surface the field reduces to zero in the $\theta = 90°$ area.

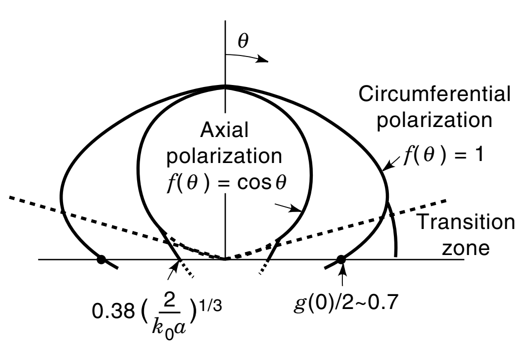

Figure 2. Approximate pattern of a thin slot on a conducting cylinder of radius a; k_0 is the free-space propagation constant. (After Ref. 6.)

Slots on Metallic Cones

Slots and slot arrays on metallic cones are found advantageous to use for missile or missilelike bodies. For efficient design of such arrays, the self- and mutual admittances must be taken into account. Theoretical and experimental investigation of slot antennas on metallic cones are discussed in Ref. 14, where the effects of scattering from a sharp tip on the mutual admittances have been investigated for pairs of circumferential and radial slots on a semi-infinite metallic cone. The base of the conical model used in the experimental study was terminated in a spherical cap to minimize scattering from the finite length of the apparatus. The two slot antennas configurations considered are shown in Fig. 3. Self- and mutual admittance expressions for pairs of slots shown in Fig. 3 have been derived by Golden, Stewart, and Pridmore-Brown (14), and the results have been confirmed by measurements. These admittance results can be immediately applied to determine the aperture voltages required for the analysis of N-element slots on cones.

In Ref. 14 the circumferential slot results illustrate interference effects between the direct coupling from slot-to-slot via the geodesic path over the conical surface and the tip back scattering. For the radial slot configuration, the results indicate negligible tip scattering effects. Golden and Stewart (15) have found that the current distribution near a slot for a sharp cone can be approximated by the distribution on an equivalent cylinder if scattering from the apex (on tip) is small. Thus, the mutual admittance between two slots can be approximately calculated by using a cylindrical model with the same local radii of curvature as the cone, provided the wave scattering from either the tip or the base region of the vehicle is negligible. The slotted cone and equivalent cylinder are shown in Fig. 4, which reveals that the cylinder has a radius equal to the radius of the circular cross section of the cone midway between the two slots antennas. For small-angle cones ($\theta_0 \sim 180°$), the radial separation of the slots on the cone can be equated to the axial separation of the slots on the equivalent cylinder.

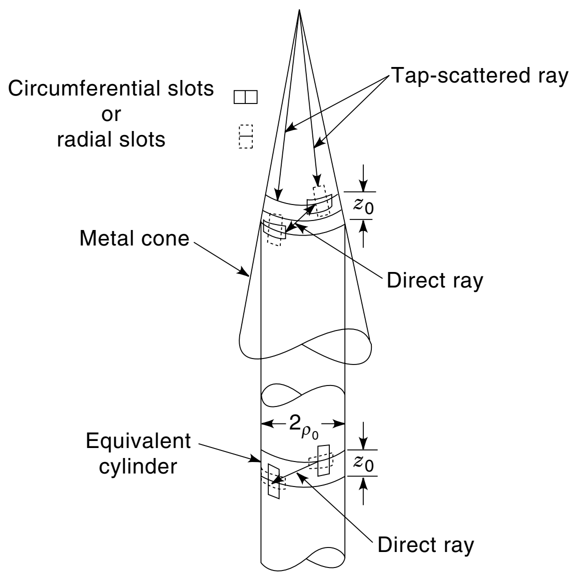

Figure 4. Slotted cone and equivalent cylinder.

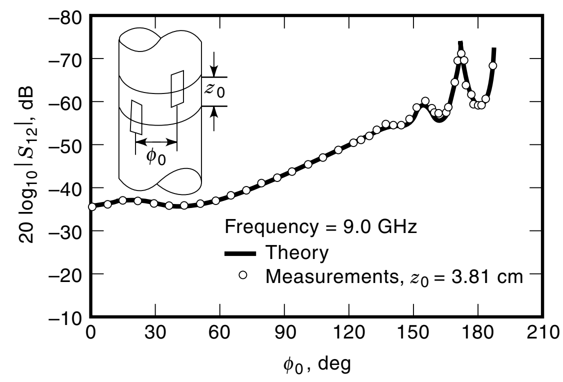

Figure 6. Mutual coupling for axial slots on cylinder, ρ_0 = 5.057 cm. (After Ref. 14.)

Mutual coupling ($|S_{12}|$ parameter) results versus azimuthal separation for two circumferential and axial slots on a cylinder are shown in Figs. 5 and 6, respectively. The mutual coupling between two radial slots on a $12 \cdot 2°$ half-angle cone is shown in Fig. 7 as a function of frequencies. Figure 8 shows the mutual coupling versus frequencies for circumferential slots on a $12 \cdot 2°$ (half-angle) cone. The results illustrate the interference effects between the direct and tip scattered components. The mutual coupling between circumferential slots on an 11° (half-angle) cone is shown in Fig. 9. Using the results given in Ref. 14, it may be concluded that for the case of circumferential slots (radial electric fields) the tip scattered portion of the azimuthal magnetic field at the slot aperture can be expressed in terms of an appropriate diffraction coefficient; in the case of radial slots (azimuthal electric fields) there is no radial component of the magnetic field in the far field of tip and therefore no contribution to the mutual admittance. More detailed results and discussions are given in Refs. 14 and 15.

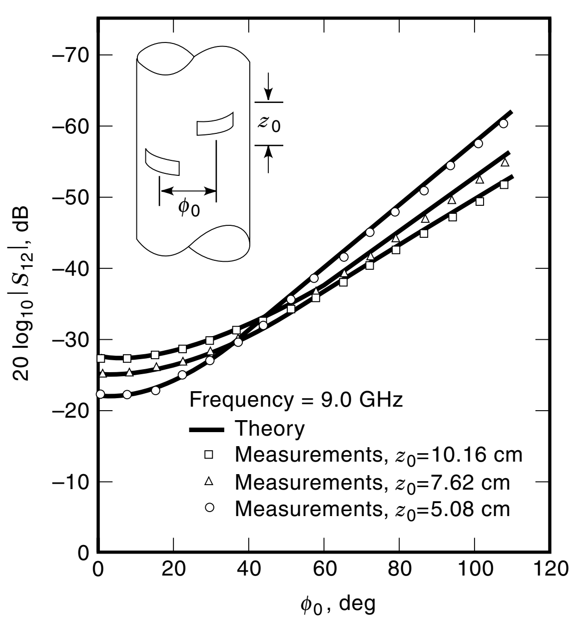

Figure 5. Mutual coupling for circumferential slots on cylinder, ρ_0 = 5.057 cm. (After Ref. 14.)

Microstrips on Curved Surfaces

Microstrip or patch is a popular low-profile, flush-mounted antenna developed in the 1970s. Detailed descriptions of the research and development of microstrip antennas can be found in Refs. 16 and 17. Such antennas generally use a metallic patch on a dielectric substrate backed by a planar ground plane, and they are excited either by a strip line or a coaxial line. The shape of the patch can be rectangular, circular, or some other shape, in general, of which the first two are the most popular. We shall mostly describe the basic rectangular patch antenna whose one dimension is $\lambda/2$ at the operating wavelength in the substance and the other dimension is slightly less than the former. Ideally, such antennas produce similar E- and H-plane patterns that have maxima in the broadside direction; generally, the polarization is linear and parallel to the patch plane but they can be designed to produce circular polarization also. For conformal applications, it is necessary to take into account the effects of nonplanar surfaces on the performance of such antennas.

Cylindrical-Rectangular Patch Antenna

The geometry of a rectangular microstrip patch antenna mounted on a conducting cylinder is shown in Fig. 10. Reso-

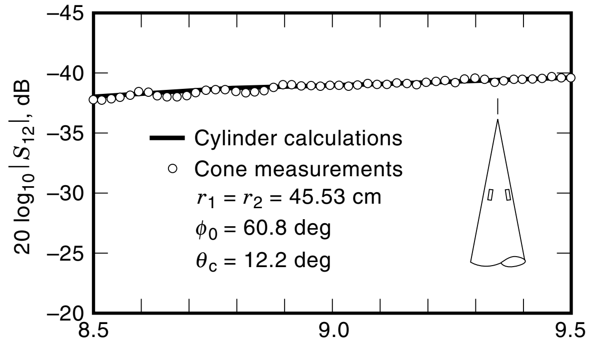

Figure 7. Mutual coupling for radial slots versus frequency, ρ_0 = 9.622 cm. (After Ref. 14.)

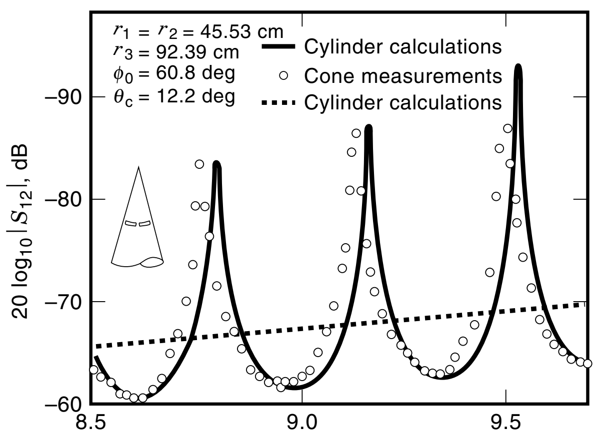

Figure 8. Mutual coupling for circumferential slots versus frequency, $\rho_0 = 9.622$ cm. (After Ref. 14.)

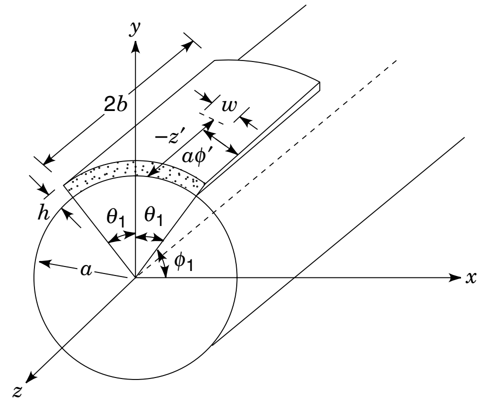

Figure 10. Geometry of a cylindrical-rectangular microstrip patch antenna.

nant frequencies and radiation characteristics of this antenna are discussed in Refs. 18 and 19. For thin substrate satisfying $h \ll a$, Luk, Lee, and Dahele (19) give the following expression for the (transverse magnetic mode with respect to ρ) TM_ρ resonant frequencies for the antenna

$$f_{mn} = \frac{c}{2\sqrt{\epsilon_r}}\left[\left(\frac{m}{2(a+h)\theta_1}\right)^2 + \left(\frac{n}{2b}\right)^2\right]^{1/2} \tag{1}$$

where c is the velocity of light in free space, ϵ_r is the dielectric constant of the substrate, and m, $n = 0, 1, 2, \ldots$, but $m = n \neq 0$. Equation (1) indicates that if the dimensions of the patch—that is, $2(a + h)\theta$ and $2b$—are fixed, the resonant frequencies of the TM_ρ modes are not affected by the curvature of the thin substrate. However, to account for fringing fields, effective values of the dimensions are to be used in Eq. (11), as mentioned by Carver and Mink (20). Luk, Lee, and Dahele (19) discuss the E- and H-plane radiation patterns produced by the antenna using $\epsilon_r = 1.06$, $\epsilon_r = 2.32$, and different values a. It is found that the patterns are not sensitive to the thickness. For a curved patch, there is significant radiation in the lower hemisphere for the TM_{01} mode; the deviation from the flat patch results increases for larger value of ϵ_r. Compared to the TM_{10} mode, there is less radiation in the lower hemisphere for the TM_{01} mode. Wong and Ke (21) describe the design of this antenna for circular polarization by using the TM_{01} and TM_{10} modes excited by a single coaxial feed located on a diagonal line and the operating frequency chosen between the two lowest frequencies f_{01} and f_{10} given by Eq. (1).

Kashiwa, Onishi, and Fukai (22) describe the application of a strip-line-fed cylindrically curved rectangular patch antenna as a small, portable antenna for mobile communication. It has been found that near the resonant frequency the real part of the input impedance approaches 50 Ω. The radiation patterns near the broadside direction are found to be similar to those of the equivalent planar antenna; however, significant differences have been found in large off-broadside directions.

Radiation patterns of a cavity-backed microstrip patch antenna on a cylindrical body of arbitrary cross section have been investigated theoretically and experimentally by Jin, Berrie, Kipp, and Lee (23). The finite-element method has been used to characterize the microstrip patch antennas, and then the reciprocity theorem is applied in conjunction with a two-dimensional method of moments to calculate the radiated field. The method can be extended to characterize the radiation patterns of conformal microstrip patch antennas on general three-dimensional bodies.

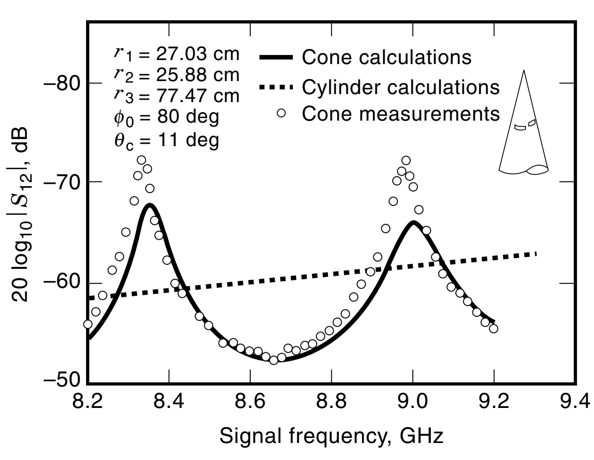

Figure 9. Mutual coupling for circumferential slots versus frequency; $\rho_0 = 5.041$ cm. (After Ref. 14.)

Microstrip Patch Antennas on Conical Surfaces

The use of microstrip antennas on conical surfaces is of interest for aerospace vehicles with portions of their bodies conically shaped. Performance of a basic rectangular patch antenna on a metallic cone has been investigated theoretically by Descardeci and Giarola (24). In the analysis the substrate thickness is assumed to be very small compared with the distance of the patch to the cone apex, and the curvature radius of the cone surface large compared with the operating wavelength. The capacitive effects and losses associated with surface wave have been neglected. Except for these assumptions, the cavity model analysis used is general and applies to any conical surface. Within the approximations made, the resonant frequency is not significantly affected by the conical surface. However, the radiation pattern is affected, with a consequent influence on the input impedance and the total quality factor. Details can be found in Ref. 24.

CONFORMAL ANTENNAS

The Omni Microstrip Antenna

The omni microstrip or spiral slot antenna discussed in Refs. 25–27 is essentially a short-circuited quarter-wavelength microstrip patch wrapped around a cylindrical surface to form a spiral, as shown in Fig. 11. The cylinder is an epoxy fiberglass dielectric, and the copper conduction are added using an electroless plating, masking, and electroplating technique. The lower end and the inside of the patch are similarly plated to form a short circuit and ground plane. The spiral slot antenna has a height and diameter of $0.06\lambda_0$ but, unlike conventional small antennas, has well-matched input voltage standing wave ratio (VSWR) of less than 2 : 1 over a 2% bandwidth at 238 MHz. The radiation patterns are similar to those of a dipole oriented parallel to the cylinder axis, and the +1 dB gain indicates an efficiency of better than 50%. The spiral slot has also been developed for 42 MHz application in which the antenna has to be contained in a $0.04\lambda_0 \times 0.15\lambda_0$ cylindrical volume.

Dielectric-Filled Edge Slot Antenna

A class of circumferential slot antennas, called the DFES antennas, that are ideally suited for conformal mounting on conducting bodies of revolution has been described by Schaubert, Jones, and Reggia (28). As shown in Fig. 12, the simplest form of the antenna consists of a disk of dielectric substrate that is copper coated on both sides and mounted between the two halves of a conducting body so that the radiating aperture coincides with the surface. The antenna is excited at the center by a coaxial line whose outer conductor is connected to the lower conducting surface, and the inner conductor is extended through the dielectric and finally connected to the conducting surface at the upper end of the substrate. The input reflection coefficients of the antenna are found to assume minimum values at some discrete frequencies, called the operating frequencies, where the antenna also radiates most efficiently. The DFES antenna can be tuned for a desired operating frequency by using a number of axially oriented passive metallic posts. The antenna without the tuning posts is referred to as the basic DFES antenna, which generally profides the highest operating frequency. By varying the number and location of the inductive posts, the operating frequency of the antenna can be tuned over a 6:1 range; instantaneous bandwidths of 3% are typical. Theory and design of basic and tuned DFES antennas mounted on a conducting cylinder have been developed and discussed by Sengupta and Martins-Camelo (29). The radiation patterns of edge-slot excited conducting bodies of revolution display a high degree of azimuthal symmetry. The radiation pattern of DFES antennas is strongly influenced by the body on which it is mounted. The patterns in Fig. 13 are typical of the performance of the antenna when mounted on a conducting cylinder.

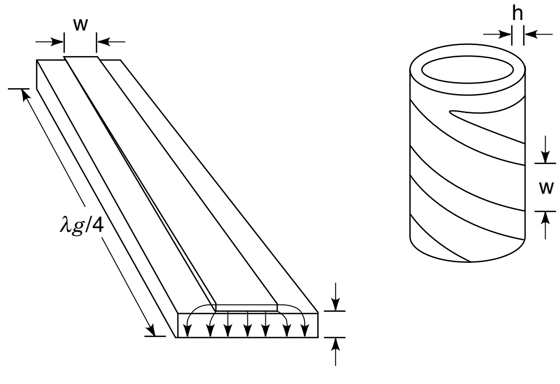

Figure 11. (a) Linear shorted $\lambda_g/4$ microstrip resonator. (b) Omni microstrip antenna: a cylindrical $\lambda/4$ microstrip resonator. (After Ref. 27.)

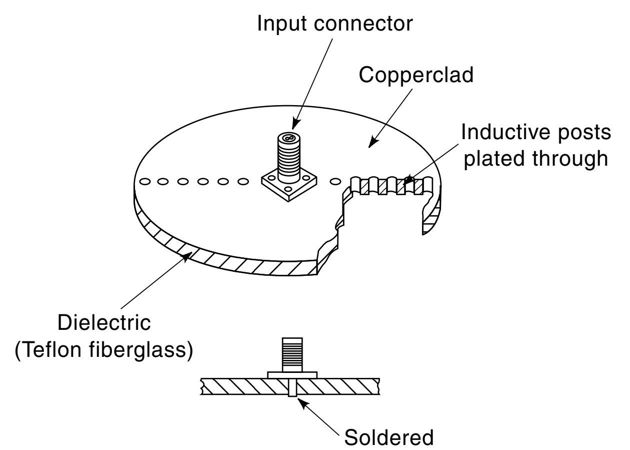

Figure 12. Two-element edge-slot antenna.

Sometimes it is not possible to place a flat disk across the body, and at times the antenna must be mounted near the top of a conical body where the diameter is not sufficient to build an antenna operating at the desired frequency. In such cases the planar disk can be deformed (symmetrically) to fit in the available space and to operate at the required frequency. A conical edge-slot antenna is described in Ref. 28, and its radiation patterns are shown in Fig. 14. The DFES antenna is a versatile and useful radiator. Because the azimuthal symmetric radiation pattern can be obtained at any desired frequency within a very wide range, system designers are not restricted in their choice of operating frequency. Also, DFES antennas can be integrated into a variety of structures because their shape can be varied to conform to the body and the available space.

Microstrip Wraparound Antennas

Microstrip wraparound antennas consisting of continuous metal strips that wrap around missiles, rockets, and satellites can provide omnidirectional coverage. Various forms of such antennas are described in Refs. 30–34. Munson (30) proposes a continuous radiator for linear polarization, as shown in Fig. 15, which shows that the microstrip feed network is a parallel (or corporate) feed network where two-way power splits are equal phase to all of the feed points. The number of power divisions can be 2, 4, 8, 16, etc. The specific number of feeds and power divisions required is dictated by the microstrip radiator. The number of feed points N_F must exceed the number of wavelengths in the dielectric in the L direction (i.e., N_F).

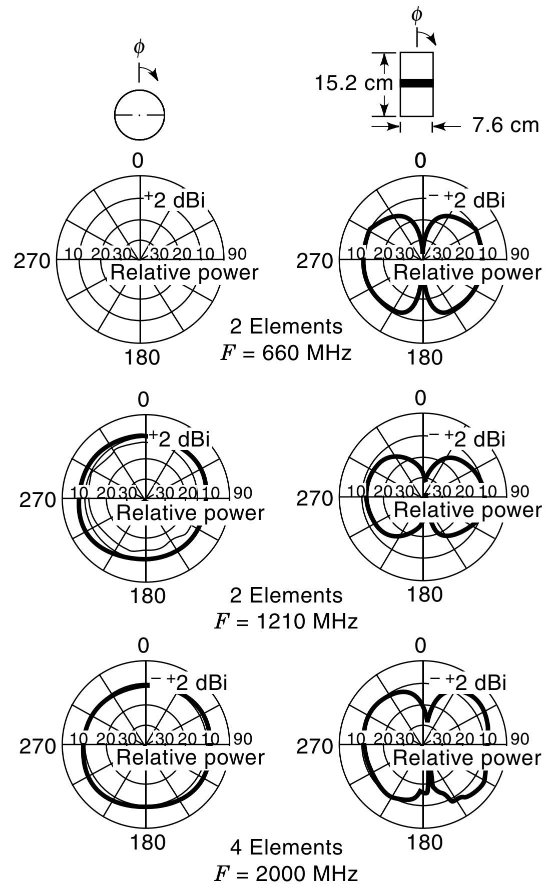

Figure 13. Radiation patterns of a 7.6 cm DFES antenna mounted on cylinder. (After Ref. 28.)

The following design relations can be used for the antenna shown in Fig. 15:

$$\lambda = \lambda_0/\sqrt{\epsilon_r} \tag{2}$$

$$w = \frac{\lambda_0}{2\sqrt{\epsilon_r}} = \lambda/2 \tag{3}$$

$$L = \pi D \tag{4}$$

$$L_D = \frac{L(\epsilon_r)^{1/2}}{\lambda_0} \tag{5}$$

$$N_{\mathrm{F}} > L_D \tag{6}$$

$$\textit{with}\ \lambda_0 = \textit{wavelength in free space} \tag{7}$$

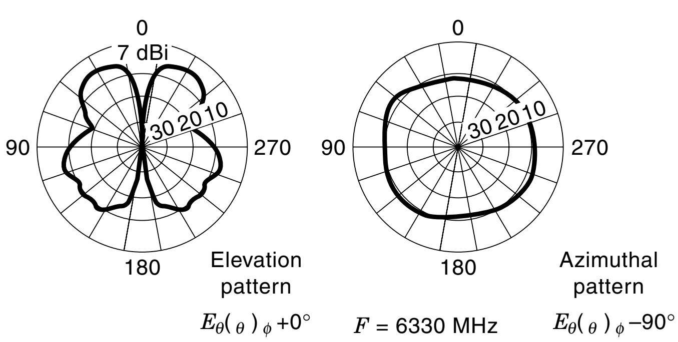

Figure 14. Radiation patterns of four-element edge-slot antenna mounted on conical base (After Ref. 28.)

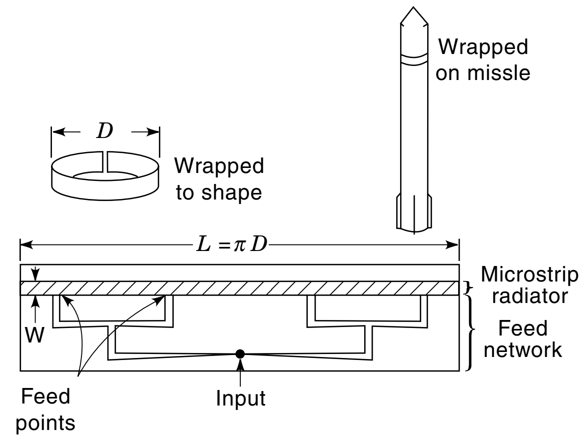

Figure 15. Microstrip wraparound antenna. (After Ref. 30.)

The pattern coverage of the omnidirectional antenna shown in Fig. 15 depends on the diameter of the missile. A typical measured E-plane pattern of a wraparound antenna mounted on an 8 in. (203 mm) cylinder given in Ref. 31 is reproduced in Fig. 16. The limiting factor in the omnidirectional coverage is a hole at the tip and tail of the missile that gets narrower as the diameter of the missile increases.

Reference 33 studies radiation patterns of wraparound microstrip antenna on a spherical body for different radii of the conducting sphere, frequencies, dielectric constant, and thickness of the dielectric. Specifically, the antenna studied consists of a metal strip of width d wrapped around a conducting sphere of radius a covered with a dielectric substrate of chosen thickness d. A φ-symmetric transverse electromagnetic mode of excitation is used. The parameter d is kept equal to half a wavelength (λ) inside the dielectric for constructive interference to occur in the broadside direction. The following

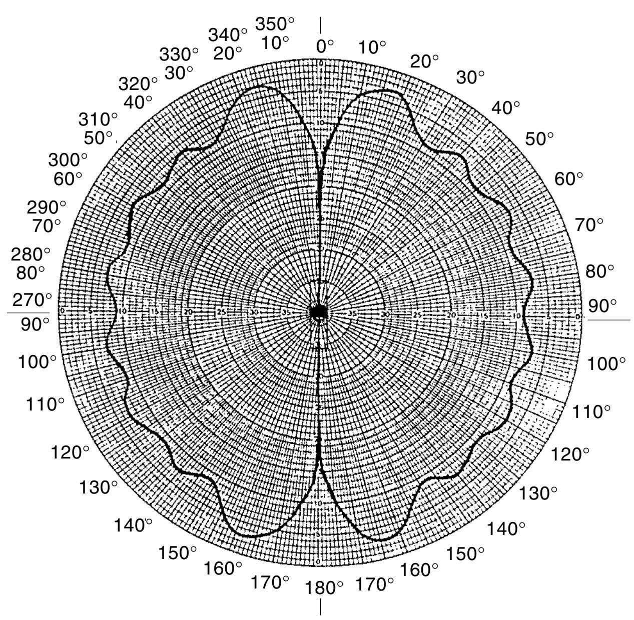

Figure 16. Measured E-plane pattern of the 8 in. (203 mm) wraparound microstrip antenna. The antenna pattern is a figure of revolution about the missile axis. (After Ref. 31.)

comments summarize the findings of the investigation reported in Ref. 33:

1. Radiation patterns are almost independent of the pressure of the patch when the radius of the sphere is much larger than the strip width.
2. The larger the radius of the sphere ($a \gg \lambda_0$), the better the omnidirectional pattern.
3. The dielectric constant ϵ_r does not have significant influence on the pattern shape. The radiation intensity tends to increase with increase of the dielectric constant.
4. The shape of the radiation patterns remains almost unchanged for different substrate thickness (h) for $h \ll \lambda_0$. However, sidelobe levels increase with increase of ϵ_r.

Radiation patterns of rectangular microstrip patches arrayed circumferentially on a circular cylinder (wraparound array) have been computed in Ref. 34. Both axial and circumferential patches, using axial and circumferential modes of excitation, respectively, have been used. In general, it has been found that the number of circumferential patches required for a given ripple in the gain pattern is considerably less than that required in the axial case, thus simplifying the feed network for the former case. Results given in Ref. 34 compared favorably with reported measurements.

A Patch Array for Aircraft

A patch array designed for an aircraft to satellite communication link is described by Sanford (35) and is shown in Fig. 17. Eight patches are mounted together with the phase shifting and feeding circuitry to scan the beam in the elevation direction. Designed for operation at 1.5 GHz, the array, including radome, is 3.6 mm thick. Element phasing was optimized for maximum multipath rejection at low scan angles and to account for the curvature of the mounting surface. Each element was pointed in a different direction and has an inherent phase error relative to the center elements. A digital computer was used to determine how the design parameters actually affect the performance of the array. The spacing of the array elements must be greater than 0.32λ (in free space) because the physical size of the radiating element on teflon fiberglass requires thin space. The spacing required to prevent the formation of grating lobes is given by

$$D \leq \frac{\lambda}{1+\sin\theta} \tag{8}$$

where D is the separation distance between the patch element, λ is the wavelength in free space, and θ is the maximum beam steering angle. For a 50° maximum steering angle, D must be less than 0.57λ.

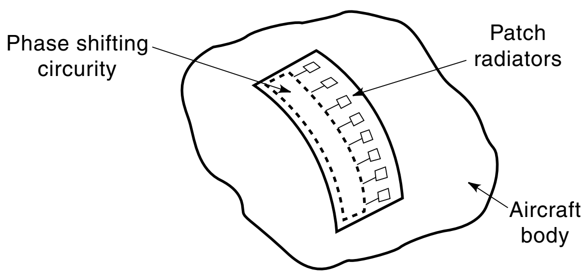

Figure 17. Conformal array for aircraft application. (After Ref. 35.)

Concentric Microstrip Ring Arrays

Bhattacharyya and Garg (36) describe the design of a concentric annular ring microstrip antenna array that can be excited by means of a single feed by interconnecting two consecutive rings with an impedance transformer. The feasibility of such an antenna is based on the observation that annular rings with different mean radii can be designed to resonate at the same frequency for the TM_{12} mode. An impedance bandwidth of about 5% for VSWR $\leq$ 2 has been reported in Ref. 36. It has been found possible to control the principal plane patterns for concentric arrays independently of each other by appropriately designing the feed system.

Saha-Misra and Chowdhury (37) describe electromagnetically fed concentric microstrip ring arrays using the log periodic principle that have been reported to have increased impedance and radiation pattern bandwidths. Specifically, circular, square, and triangular concentric rings have been investigated. Generally, these antennas work at multiple bands of frequencies with some bands having larger bandwidths than standard microstrip antennas. With a nonuniformly spaced concentric annular ring array, almost 20% bandwidth for VSWR $\leq$ 2 has been reported. A planar, wideband feed for a slot spiral antenna has been described by Nurnberger and Volakis (38). The antenna has been developed for operation at very high frequency (VHF) frequencies. In contrast to most traditional printed spiral antenna designs, the one reported in Ref. 38 incorporates a completely planar spiral microstrip balun feed, thereby making it attractive for a variety of conformal applications.

CONFORMAL ARRAYS

Antenna arrays conforming to a nonplanar surface are suitable and may even be a requirement for a number of applications. For example, phased arrays of flush-mounted elements conformally mounted on the surface of an aircraft or missile reduce the aerodynamic drag and hence are preferable. Also, in some cases a nonplanar array surface may provide some natural advantage for broad-beam coverage in space. Spherical, cylindrical, and conical arrays have been developed for ground, airborne, and missile applications. We shall consider here the class of conformal arrays where the radiating surface is nonplanar with a radius of curvature large compared to the operating wavelength. Conformal arrays that are highly curved are generally difficult to design because of the following reason (1,3,8,4):

1. Array elements point in different directions and so it is often necessary to switch off those elements that radiate primarily away from the desired direction of radiation.

This, in turn, requires more sophisticated switching mechanisms for activation of elements.

2. The fact that element patterns cannot be factored out of the total radiation pattern makes the analysis and synthesis of such antennas more complicated.
3. Mutual coupling effects can be very severe and difficult to ascertain.
4. Nonplanar arrangement of elements may give rise to severe cross-polarization effects.

Spherical Arrays

Certain applications require phased arrays capable of steering the beam over a complete hemisphere. For this requirement a spherical array surface seems to provide some natural advantage for beam steering. Schrank (39) discusses the manner in which an array of radiating elements placed on a sphere provides a natural configuration for obtaining hemispherical coverage with nearly identical highly directive beams. A spherical phased array consisting of circularly polarized flat spiral antenna elements has been developed by Sengupta, Smith, and Larson (40) and Sengupta, Ferris, and Smith (41). Theoretical design and other considerations are given in Ref. 42, and experimental fabrication and results are given in Ref. 41. As described in Ref. 40, a special element distribution was obtained from the consideration of icosahedron geometry resulting in a best possible uniformity of element spacing. It was found that the array could operate with widely spaced elements. The special element distribution developed for this purpose considerably suppressed the grating lobes in the pattern and thereby made the array significantly broadband. Figure 18 shows the icosahedron geometry of element locations on a spherical surface. The choice of circularly polarized elements made the antenna beam retain its circular polarization fairly well over the entire range of beam steering directions (39,40). Experimental results given in Ref. 41 demonstrate the capability of a spherical array of 16 flat spiral antennas over a frequency range 0.6 to 3 GHz. The work reported in Ref. 41 used manual control of phase and illuminated aperture area; consequently, the results obtained were limited in scope. However, with the availability of modern sophisticated computer control mechanisms, it seems that such spherical arrays could provide almost complete hemispherical phased coverage over a broad band.

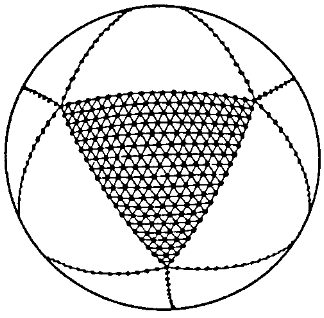

Figure 18. Icosahedron geometry of element locations. (After Ref. 39.)

Cylindrical Arrays

Conformal elements like microstrips and slots arrayed around the circumference of large metal cylinders have been used to obtain omnidirectional pattern coverage. Such coverage may also be obtained with the help of wraparound antenna, as discussed earlier. References 42–46 show that an array of slots equally spaced around the circumference of a cylinder can produce a pattern with very low ripple. Croswell and Knop (43) have obtained extensive numerical data using realistic patterns for slots on perfectly conducting planes. In such arrays the design parameters are the numbers of elements, radiating elements, and feed network. The number of elements is chosen to provide a nearly omnidirectional pattern; the minimum number of elements is decided by the allowed amplitude ripple. The evaluation of the amplitude ripple can be given in terms of the fluctuation, which is defined as the ratio of maximum $|F|$ to minimum $|F|$, where F is the total far-field pattern of an S-element circular array and is given by (42)

$$F = S\sum_{n=0}^{N} A_n(-j)^n \frac{d^n}{d_{z^n}}[J_0(z) + 2(j)SJ_S(z)\cos S\varphi] \tag{9}$$

where $J_S(z)$ is the Bessel function of the first kind of order S, $z = k_0a\,\sin\theta$; k_0 is the free-space wave number; a is the radius of the circular array; θ, φ are the usual coordinates, and the z-axis is the axis of the cylinder; and $N \leq S$.

The preceding expression assumes that the single element pattern $f(\varphi^1)$ can be expressed by a Fourier cosine series

$$f(\varphi') = \sum_{n=0}^{\infty} A_n \cos^n \varphi' \tag{10}$$

A practical single element pattern can be approximated by

$$f(\varphi') = \begin{cases} (1+\cos\varphi'/2)/2 \\ (2+3\cos\varphi' + \cos 2\varphi')/6 \end{cases} \tag{11}$$

Pattern fluctuations as a function of size of cylinder and number of elements for the preceding two single-element patterns are given in Ref. 43. Cylindrical phased arrays, where selected sections are illuminated to provide a beam in a certain direction, are sometimes found advantageous to use for some requirements. Sophisticated types of electronic switches for such circular arrays are based on a concept originally proposed by Shelton (45) and developed by Sheleg (46). The antenna uses a Butler matrix-fed circular array with fixed phase shifters to execute current modes around the array and variable phase shifters to provide continuous scanning of the radiated beam over 360°. The operation was experimentally demonstrated with a 32-dipole circular array.

The principles involved in scanning a multimode array are readily seen by considering a continuous distribution of current, as described by Sheleg (47). Figure 19 shows the configuration of a continuous cylindrical sheet of vertical current elements around a vertical conducting cylinder of radius a. Referring to Fig. 19, consider a current distribution $I(\alpha)$ to be the sum of a finite number of continuous current modes $I_n e^{jn\alpha}$ with $-N \leq n \leq N$. The radiation pattern for $I(\alpha) = I_n e^{jn\alpha}$ is then given by

$$E(\varphi) = \sum_{n=-N}^{N} C_n e^{in\varphi} \tag{12}$$

where C_n are complex constants given by

$$C_n = 2\pi K j^n I_n J_n \left(\frac{2\pi a}{\lambda}\right) \tag{13}$$

with K a constant, λ being the wavelength of operation, and J_n being the Bessel function defined earlier. If, in the antenna being considered, it is desired that the pattern mode be equal in magnitude and be in phase at $\varphi = 0$, the excitation of the current modes must be

$$I_n = \frac{1}{2\pi K j^n J_n \left(\frac{2\pi a}{\lambda}\right)} \tag{14}$$

Under this condition, the radiation pattern is given by

$$E(\varphi) = \sum_{n=-N}^{N} e^{jn\varphi} = \sin\frac{\left(\frac{2N+1}{2}\varphi\right)}{\sin\frac{\varphi}{2}} \tag{15}$$

If the phase difference between the adjacent modes is φ_0 (i.e., multiply I_n by $e^{-jn\varphi}$], the resultant radiation pattern is

$$E(\varphi) = \frac{\sin[(2N+1)(\varphi-\varphi_0)/2]}{\sin[(\varphi-\varphi_0)/2]} \tag{16}$$

which indicates a beam in the φ_0 direction. As described by Sheleg (46), it was possible to excite simultaneously and independently all the modes both positive and negative n, from 0 to $N/2$, by connecting a single ring on N elements to the outputs of a Bulter matrix. A schematic diagram of a scanning

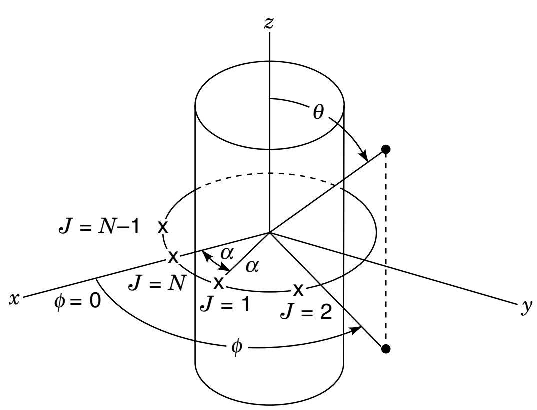

Figure 19. Coordinates for continuous cylindrical sheet of vertical current elements.

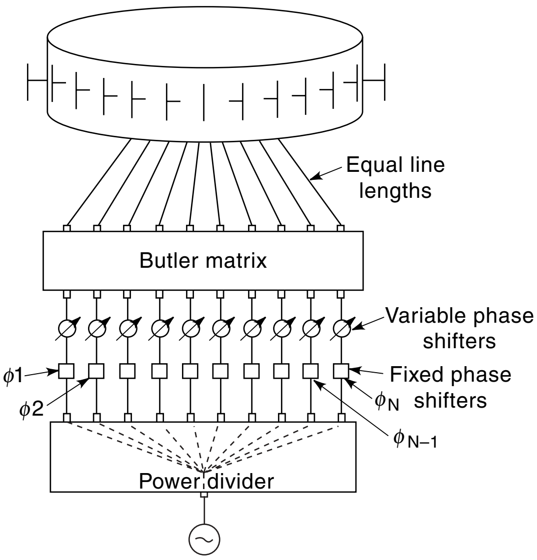

Figure 20. Schematic diagram of scanning multimode array. (After Ref. 46.)

multimode array is shown in Fig. 20. The desired phase and amplitude distribution is established over the inputs of the Bulter matrix by fixed phase shifts and a corporate structure. Once the pencil beam pattern is formed at some azimuth angle, it is scanned just as in a linear array; the mode amplitudes are held fixed and a linear phase progression is set up on the mode inputs by operating the variable phase shifters.

Conical Array

Kummer (1) discusses a number of difficulties associated with antenna pattern synthesis utilizing conical surfaces. An array on a conical surface generally looks different at different aspect angles; also, the geometry is such that all elements do not contribute equally to the main beam direction, thereby causing cross-polarization problems. In spite of this, for their obvious applications to missile and other similar vehicles, conical arrays have been considered for conformal array development. Theoretical and experimental investigations of various aspects of conical arrays are discussed in Refs. 15, 47, and 48. The experimental studies of Munger 48) provide some data on the characteristics of several conical arrays. Balzano and Dowling (47) developed an effective method to evaluate the pattern of elements in a conical array. The method takes into account the mutual coupling between array elements and aperture matching conditions. By properly matching the array aperture, the radiation in a certain direction can be substantially increased, thus allowing the designer to meet specific design goals in the application of conical arrays to airborne or missile-borne systems. Moreover, it has been shown that in some cases, the element pattern can be approximated by much simpler planar and cylindrical models.

BIBLIOGRAPHY

1. W. H. Kummer, Preface, *IEEE Trans. Antennas Propag.,* **AP-22**: 1–3, 1974.
2. C. A. Balanis, *Antenna Theory,* 2nd ed., New York: Wiley, 1997.

3. R. C. Johnson and H. Jasik, (eds.), *Antenna Engineering Handbook,* 2nd ed., New York: McGraw-Hill, 1984.
4. R. C. Hansen, *Significant Phased Array Papers,* Dedham, MA: Artech House, 1973.
5. Y. T. Lo and S. W. Lee, (eds.), *Antenna Handbook: Theory, Applications, and Design,* New York: Van Nostrand Reinhold, 1988.
6. R. J. Mailloux, *Phased Array Antenna Handbook,* Boston: Artech House, 1994.
7. W. H. Kummer, guest editor, Special Issue on Conformal Arrays, *IEEE Trans. Antennas Propag.,* **AP-22**: 1–150, 1974.
8. R. C. Hansen, *Microwave Scanning Antennas,* Vols. 1-III, New York: Academic Press, 1964.
9. P. H. Pathak and R. G. Kouyoumjian, An analysis of the radiation from aperture in curved surfaces by the geometrical theory of diffraction, *Proc. IEEE,* **62**: 1438–1447, 1974.
10. P. H. Pathak et al., A uniform GTD solution for the radiation from sources on a curvex surface, *IEEE Trans. Antennas Propag.* **AP-29**: 602–622, 1981.
11. W. D. Burnside, R. J. Marhefka, and C. L. Yu, Roll plane analysis of on-aircraft antennas, *IEEE Trans. Antennas Propag.,* **AP-21**: 780–786, 1973.
12. W. D. Burnside et al., A Study of KC-135 aircraft antenna patterns, *IEEE Trans. Antennas Propag.,* **AP-23**: 309–316, 1975.
13. R. J. Mailloux, Conformal and low-profile arrays, in Ref. 3.
14. K. E. Golden, G. E. Stewart, and D. C. Pridmore-Brown, Approximation techniques for the mutual admittance of slot antennas on metallic cones, *IEEE Trans. Antennas Propag.,* **AP-22**: 43–48, 1974.
15. K. E. Golden and G. F. Stewart, Self and mutual admittance of rectangular slot antennas in the presence of inhomogeneous plasma layer, *IEEE Trans. Antennas Propag.,* **AP-17**: 763–771, 1969.
16. D. C. Chang, (ed.), *IEEE Trans. Antennas Propag.,* **AP-29**: 1–182, 1981.
17. I. J. Bahl and P. Bhartia, *Microstrip Antennas,* Norwood, MA: Artech House, 1980.
18. C. M. Krowne, Cylindrical-rectangular microstrip antenna, *IEEE Trans. Antennas Propag.,* **AP-31**: 194–199, 1983.
19. K.-M. Luk, K.-F. Lee, and J. S. Dahele, Analysis of the cylindrical-rectangular patch antenna, *IEEE Trans. Antennas Propag.,* **AP-37**: 143–147, 1989.
20. K. R. Carver and J. W. Mink, Microstrip antenna technology, *IEEE Trans. Antennas Propag.,* **AP-29**: 2–24, 1981.
21. K.-L. Wong and S.-Y. Ke, Cylindrical-rectangular microstrip for circular polarization, *IEEE Trans. Antennas Propag.,* **AP-41**: 246–249, 1993.
22. T. Kashiwa, T. Onishi, and I. Fukai, Analysis of microstrip antennas on a curved surface using the conformal grids FD-TD method, *IEEE Trans. Antennas Propag.,* **AP-42**: 423–427, 1994.
23. J. M. Jin et al., Calculation of radiation patterns of microstrip antennas on cylindrical bodies of arbitrary cross section, *IEEE Trans. Propag.,* **AP-45**: 126–132, 1997.
24. J. R. Descardeci and A. J. Giarola, Microstrip antenna on a conical surface, *IEEE Trans. Antennas Propag.,* **AP-40**: 460–463, 1992.
25. H. S. Jones, *Design of dielectric-loaded circumferential slot antennas of arbitrary size for conical and cylindrical bodies,* Report HDL-TR-1684, Hary Diamond Laboratories, Adelphi, MD, 1974.
26. D. H. Schaubert, A. R. Sindons, and F. G. Farrar, The spiral slot: a unique microstrip antenna, *Proc. 1978 Antenna Applic. Symp.,* Univ. of Illinois Allerton Conf., Hary Diamond Laboratories, October 1978.
27. A. D. Krall et al., The omni microstrip antenna: a new small antenna, *IEEE Trans. Antennas Propag.,* **AP-27**: 850–853, 1979.
28. D. H. Schaubert, H. S. Jones, and F. Reggia, Conformal dielectric-filled edge-slot antennas with inductive-post turning, *IEEE Trans. Antennas Propag.,* **AP-27**: 713–716, 1979.
29. D. L. Sengupta and L. F. Martins-Camelo, Theory of dielectric-filled edge-slot antennas, *IEEE Trans. Antennas Propag.,* **AP-28**: 481–490, 1980.
30. K. F. Munson, Conformal microstrip antennas and microstrip phased arrays, *IEEE Trans. Antennas Propag.,* **AP-22**: 74–78, 1974.
31. R. F. Munson, Omnidirectional microstrip arrays, pp. 7-19, 7-21 of Ref. 3.
32. S. B. D. A. Fonseca and A. J. Giarola, Analysis of microstrip wraparound antennas using dyadic Green's functions, *IEEE Trans. Antennas Propag.,* **AP-31**: 248–253, 1983.
33. A. Das, S. K. Das, and M.-S. Narasimhan, Radiation characteristics of wraparound microstrip antenna on spherical body, *IEEE Trans. Antennas Propag.,* **AP-39**: 1031–1034, 1991.
34. I. Jayakumar et al., A conformal cylindrical microstrip array for producing omnidirectional radiation pattern, *IEEE Trans. Antennas Propag.,* **AP-34**: 1258–1261, 1986.
35. G. G. Sanford, Conformal microstrip phased array for aircraft tests with ATS-6, *IEEE Trans. Antennas Propag.,* **AP-26**: 642–646, 1978.
36. A. K. Bhattacharyya and R. Garg, Input impedance of annular ring microstrip antenna using circuit theory approach, *IEEE Trans. Antennas Propag.,* **AP-33**: 369–374, 1985.
37. I. Saha-Misra and S. K. Chowdhury, Concentric microstrip ring antenna: theory and experiment, *J. Electromagn. Wave Applications,* **10**: 439–450, 1996.
38. M. W. Nurnberger and J. L. Volakis, A new planar feed for slot spiral antennas, *IEEE Trans. Antennas Propag.,* **AP-44**: 130–131, 1996.
39. H. E. Schrank, Basic theoretical aspects of spherical phased arrays, in A. A. Oliner and G. H. Knitted (eds.), *Phased Array Antennas,* Dedham, MA: Artech House, pp. 323–327, 1972.
40. D. L. Sengupta, T. M. Smith, and R. W. Larson, Radiation characteristics of spherical array of circularly polarized elements, *IEEE Trans. Antennas Propag.,* **AP-16**: 1–7, 1968.
41. D. L. Sengupta, J. E. Ferris, and T. M. Smith, Experimental study of a spherical array of circularly polarized elements, *Proc. IEEE,* **56**: 2048–2051, 1968.
42. T. S. Chu, On the use of uniform circular arrays to obtain omnidirectional patterns, *IEEE Trans. Antennas Propag.,* **AP-7**: 436–438, 1959.
43. W. F. Croswell and C. M. Knop, On the use of an array of circumferential slots on a large cylinder as a omnidirectional antenna, *IEEE Trans Antennas Propag.,* **AP-14**: 394–396, 1966.
44. W. F. Croswell and C. R. Cockrell, An omnidirectional microwave antenna for use on spacecraft, *IEEE Trans. Antennas Propag.,* **AP-17**: 459–466, 1969.
45. P. Shelton, Application of hybrid matrices to various multimode and multibeam antenna systems, *IEEE Washington Chapter P GAP Meet.,* March 1965.
46. B. Sheleg, A matrix-fed circular array for continuous scanning, *Proc. IEEE,* **56**: 2016–2027, 1968.
47. Q. Balzano and T. B. Dowling, Mutual coupling analysis of arrays of apertures on cones, *IEEE Trans. Antennas Propag.,* **AP-22**: 92–97, 1974.
48. A. D. Munger et al., Conical array studies, *IEEE Trans. Antennas Propag.,* **AP-22**: 35–42, 1974.

DIPAK L. SENGUPTA
University of Detroit Mercy